

Supporting Information

A Biomimetic Platform to Study the Interactions of Bioelectroactive Molecules with Lipid Nanodomains

Joaquim T. Marquês, Ana S. Viana*, Rodrigo F. M. de Almeida*

Centro de Química e Bioquímica, Faculdade de Ciências, Universidade de Lisboa, Ed. C8, Campo Grande, 1749-016 Lisboa, Portugal

I. Reductive desorption of MUA and Cys monolayers and assessment of Cys SAM global charge

Surface coverage of both MUA and Cys SAM was determined by reductive desorption and the electrochemical behavior of two differently charged redox probes, $[K_3Fe(CN)_6]$ and $[Ru(NH_3)_6]Cl_3$, was employed to assess the global charge of the Cys SAM.

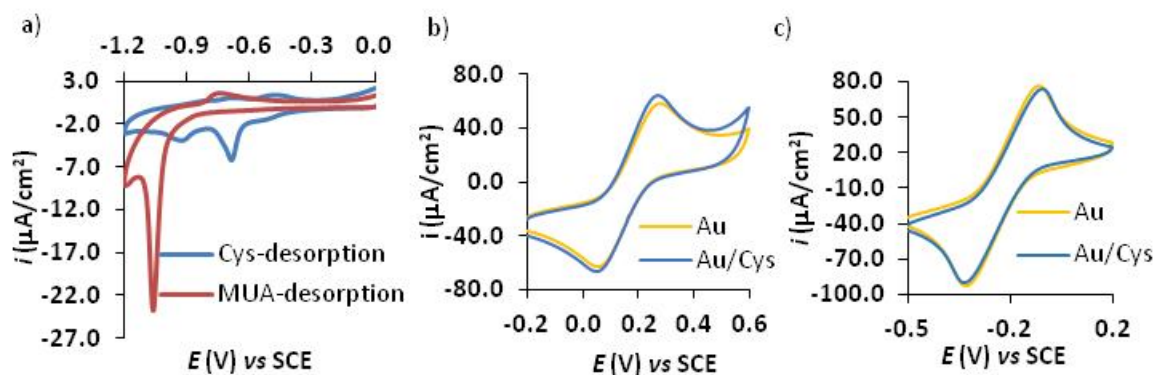


Figure S1 – a) Reductive desorption of L-cysteine and 11-mercaptoundecanoic acid self-assembled on Au (111) performed in 0.1 M NaOH at a scan rate of 20 mV/s. b) $[K_3Fe(CN)_6]$ redox process on a bare and Cys-modified gold surface and c) $[Ru(NH_3)_6]Cl_3$ redox process on a bare and Cys-modified gold surface measured in HEPES buffer 50 mM, pH 7.4, at a scan rate of 50 mV/s.

II. a) Real-time monitoring of lipid vesicles adsorption on modified gold surfaces.

With the purpose of assessing if modified electrodes with Cys are effective towards lipids' polar head group adsorption, we followed the real-time adsorption of lipid vesicles composed of DOPC/DPPE/Chol (2:2:1) on modified gold surfaces. Taking into account that substrate roughness is one of the factors playing an important role in terms of SLB formation¹, and both QCM and SPR electrodes present a higher roughness compared to Au (111) it is most likely that substrate topography will affect vesicle fusion or rupture required for planar SLB formation. Therefore, for the intended purpose of evaluating the extension and kinetics of vesicles adsorption, both QCM and SPR are quite suitable techniques. The two experimental approaches revealed that lipid vesicles interact to a similar extent with both MUA and Cys modified gold surface considering that an identical amount of lipid material is being adsorbed on top of each

electrode surface (Figure S2). Moreover, both QCM (Figure S2a) and SPR (Figure S2b) revealed that the interaction occurs with almost coincident kinetics for each SAM. Thus it is shown that a long compact monolayer is not necessary for efficient vesicle adsorption. Single lipid bilayer formation could not be detected on top of any of the electrodes used whether for QCM or SPR. The total mass adsorbing on QCM gold electrode was $\sim 2.41 \times 10^{-6} \text{ g/cm}^2$ and $\sim 2.42 \times 10^{-6} \text{ g/cm}^2$ for the MUA and Cys modified electrodes, respectively, whereas a mass of $4.4 \times 10^{-7} \text{ g/cm}^2$ would be expected for the formation of a single lipid bilayer arrangement, as described in detail in section II.b). The difference between the calculated and measured values clearly shows that most probably a large amount of intact vesicles is being adsorbed on the surface. For both surface modifications, the presence of calcium in the buffer containing the lipid vesicles in suspension was required, since in its absence no significant adsorption to the surface took place (data not shown). More importantly, for the type of gold used in these experiments, a previous surface modification with SAM proved to be crucial to drive a favorable interaction between the lipid and the surface, as in bare Au only the deposition of a sub-monolayer ($1.79 \times 10^{-7} \text{ g/cm}^2$) was detected (Figure S2a).

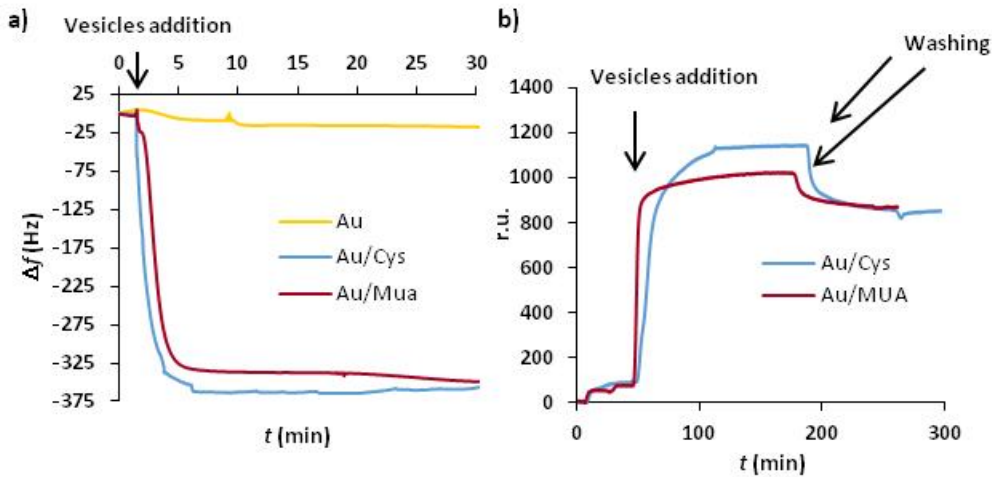


Figure S2 – Real-time monitoring of lipid vesicles adsorption onto bare, Cys- and MUA- modified gold surfaces by a) Quartz Crystal Microbalance and b) Surface Plasmon Resonance. The experiments were conducted in HEPES buffer containing 150 mM NaCl and 5 mM CaCl_2 or containing only 5mM CaCl_2 for MUA or Cys modified gold surfaces, respectively. The experiments were carried out with DPPC/DOPC/chol (2:2:1 mol ratio) lipid vesicles.

b) Determination of adsorbed mass by Quartz Crystal Microbalance

The amount of lipid deposited on top of bare and modified QCM electrodes was computed using the change in frequency of the quartz crystal upon a given mass variation which is given by Sauerbrey's equation²,

$$\Delta f = -\frac{2f_0^2}{A\sqrt{\rho_q\mu_q}}\Delta m \quad (\text{Eq. S1})$$

where Δf is the frequency variation in Hz, f_0^2 stands for the resonant frequency, which in the present case was determined by the manufacturer to be 8 MHz, A is the piezoelectroactive area of the crystal, ρ_q corresponds to the density of quartz which is 2.648 g/cm^3 , μ_q is the shear modulus of quartz for an AT-cut crystal which has a value of $2.947 \times 10^{11} \text{ g/cm} \cdot \text{s}^2$ and Δm expresses the

change in mass. Considering all the parameters stated above, our QCM exhibits a sensitivity of 6.9×10^{-9} g/Hz. Below, in table S1, a compilation of all the values calculated from QCM data is presented.

Table S1 – QCM frequency shift (Δf) and mass change (Δm and $\Delta m/A$) for bare and MUA- and Cys modified gold electrodes. The estimated values for the formation of a ternary lipid bilayer are also shown.

System	Δf (Hz)	Δm (g)	$\Delta m/A$ (g/cm ²)	Lipid arrangement
Au	-26	3.5×10^{-8}	1.8×10^{-7}	Sub-monolayer
Au/MUA	-348	4.7×10^{-7}	2.4×10^{-6}	Vesicles
Au/Cys	-350	4.7×10^{-7}	2.4×10^{-6}	Vesicles
Theoretical	-64	8.6×10^{-8}	4.4×10^{-7}	Planar bilayer
Au/SLB				

In table S1 the value estimated for the mass of lipid for a planar and continuous lipid bilayer arrangement on the gold surface is also presented. This value was obtained taking into account both the molar proportion and the area per molecule (A) of each lipid and lipid phase– liquid ordered (l_o) and liquid disordered (l_d). The mol fraction and composition of each phase were taken from the phase diagram for this mixture and the tie-line containing the 2:2:1 molar proportion³. The phase l_o corresponds to ~ 40 mol % of the system with a lipid composition of ca. 63% DPPC, 33% Chol and 4% DOPC (mol%), while the remaining 60 mol% are in the l_d phase with a lipid composition of 65% DOPC, 25% DPPC and 10% Chol. For these lipid proportions, in l_o the area per lipid is around 43 \AA^2 ⁴ while in l_d the area per lipid is close to 60 \AA^2 ⁵. Considering the following definitions:

$$a_{ld} = \frac{A_{ld}}{N_{ld}}$$

$$a_{lo} = \frac{A_{lo}}{N_{lo}}$$

$$A_t = A_{ld} + A_{lo}$$

$$N_{ld} = \frac{3}{2}N_{lo}$$

where A_t is the total area, a_{ld} and a_{lo} are the area per lipid, A_{ld} and A_{lo} stand for the total area, and N_{ld} and N_{lo} express the total number of molecules in the l_d and l_o phase, respectively, we estimated that the area fraction for the l_o phase is close to 32% while for the l_d is 68%, as shown next. Admitting a total electrode area (A_t) of 1 cm^2 :

$$1 - A_{lo} = A_{ld} \Leftrightarrow 1 - A_{lo} = a_{ld} \times \frac{3}{2}N_{lo} \Leftrightarrow \frac{1 - A_{lo}}{\frac{3}{2}\left(\frac{A_{lo}}{a_{lo}}\right)} = a_{ld} \Leftrightarrow a_{lo} = \frac{3}{2}a_{ld}A_{lo} + A_{lo}a_{lo} \Leftrightarrow$$

$$\Leftrightarrow A_{lo} = \frac{a_{lo}}{\frac{3}{2}a_{ld} + a_{lo}} \Leftrightarrow A_{lo} = 0.32 \text{ cm}^2$$

Consequently, $A_{ld} = 0.68 \text{ cm}^2$

Knowing that,

$$M(\text{DOPC}) = 786.15 \text{ g/mol}$$

$$M(\text{DPPC}) = 734.05 \text{ g/mol}$$

$$M(\text{Chol}) = 386.66 \text{ g/mol:}$$

$$N_{ld} = \frac{A_{ld}}{a_{ld}} \Leftrightarrow N_{ld} = \frac{6.8 \times 10^{15}}{60} = 1.13 \times 10^{14} \text{ molecules.}$$

$$n = \frac{1.13 \times 10^{14}}{6.022 \times 10^{23}} = 1.88 \times 10^{-10} \text{ mol.}$$

$$m_{ld} = 1.88 \times 10^{-10} \times ((0.9 \times 786.15) + (0.1 \times 386.66)) = 1.4 \times 10^{-7} \text{ g}$$

$$N_{lo} = \frac{A_{lo}}{a_{lo}} \Leftrightarrow N_{lo} = \frac{3.2 \times 10^{15}}{43} = 7.44 \times 10^{13} \text{ molecules of } l_o.$$

$$n = \frac{7.44 \times 10^{13}}{6.022 \times 10^{23}} = 1.23 \times 10^{-10} \text{ mol of } l_o.$$

$$m_{lo} = 1.24 \times 10^{-10} \times ((0.7 \times 734.05) + (0.3 \times 386.66)) = 7.9 \times 10^{-8} \text{ g}$$

For a bilayer arrangement the actual mass would be the double of those values and hence the total mass would correspond to, approximately, $4.4 \times 10^{-7} \text{ g/cm}^2$.

III. Determination of partition coefficient of epinephrine and its membrane-bound state anisotropy

Epinephrine surface coverage, determined in cyclic voltammetric experiments, and the total number of lipid moles present in an area of 1 cm^2 were used to estimate the mole-fraction partition coefficient⁶ of epinephrine (K_p):

$$K_p = \frac{\frac{n_L^E}{n_L}}{\frac{n_w^E}{n_w}} \quad (\text{Eq. S2})$$

where n_w and n_L are the amount (in mole) of water and lipid in each sample, and n_i^E is the amount of epinephrine molecules present in each phase ($i = w$, aqueous phase; $i = L$, lipid phase, respectively). Considering the surface coverage of epinephrine for the fluid system ($\Gamma = 9.36 \times 10^{-11} \text{ mol/cm}^2$) and the amount of DOPC (molar volume at 20°C taken from⁷) in 1 cm^2 ($4.48 \times 10^{-10} \text{ mol}$), $K_p = 1.13 \times 10^4$. For a gel phase DPPC membrane (molar volume taken from⁷) K_p will be 2.8×10^3 .

With these K_p estimations it is, then, possible to calculate a fraction of epinephrine bound to the membrane⁶ (x_L) in the fluorescence spectroscopy studies, both for the 1 mM and 3 mM lipid experiments:

$$x_w = \frac{[W]}{[W] + K_p[L]} \quad (\text{Eq. S3})$$

where $[L]$ and $[W]$ are the lipid and water concentration, respectively. In the case of fluid DOPC, for 1 mM of lipid $x_w = 0.827$ and for 3 mM of lipid $x_w = 0.615$. Since the total concentration of epinephrine was the same in every sample:

$$I = \sum x_i I_i \quad (\text{Eq. S4})$$

where I is the steady-state fluorescence intensity of epinephrine, I_i is the limiting value characteristic of either free or membrane-bound states and x_i is the fractional population of each species in a sample ($i = w$, aqueous phase; $i = L$, lipid phase)⁶. Thus, plotting the fluorescence intensity data obtained for epinephrine in each condition (solution, 1 mM and 3 mM of lipid – Figure 4b in the main article) *versus* mole fraction in solution we can find the fluorescence intensity for epinephrine when totally bound to the membrane, which corresponds to the extrapolation of such representation to zero (only membrane-bound form). The R^2 of this data is 0.99, yielding $I_L = 9.1 \times 10^6$. The fraction of light (f_i) coming from epinephrine in its free and membrane-bound states can be retrieved from the following equation:

$$f_i = \frac{x_i I_i}{I} \quad (\text{Eq. S5})$$

The steady-state anisotropy, $\langle r \rangle$, of epinephrine can, then, be expressed as a function of the contribution of the anisotropy from free, $\langle r \rangle_w$, and membrane-bound, $\langle r \rangle_L$, epinephrine weighted by the fraction of light coming from both free (f_w) and membrane-bound (f_L) forms (Weber's and Jablonski's additivity law of anisotropy⁸):

$$\langle r \rangle = \langle r \rangle_w f_w + \langle r \rangle_L f_L \quad (\text{Eq. S6})$$

From the data in Figure 4, for the fluid system $I_w = 1.2 \times 10^7$ and $\langle r \rangle_w = 0.0175$. Using the anisotropy values experimentally determined for 1mM and 3 mM of lipid, it is possible to retrieve $\langle r \rangle_L$. The values obtained are 0.01387 and 0.01056, respectively. Thus the anisotropy of epinephrine bound to a fluid membrane is -0.0075. For the other systems the uncertainty is larger due to the lower partition coefficients. However, it was clear that in all those cases a negative value of anisotropy for membrane bound epinephrine can be estimated and the values range between -0.1 and -0.2. These are within the range of physically feasible values for steady-state fluorescence anisotropy for a fluorophore with perpendicular absorption and emission transition dipole moments⁹. Moreover, these values are more negative than for the fluid DOPC, in agreement with the fact that the fraction of epinephrine in the membrane bound form is lower (smaller K_p) and the decrease in anisotropy is more pronounced. This shows that the hormone is more immobilized in these systems as compared to the fluid DOPC bilayer membrane, which is expected taking into account that the DOPC bilayer is the most disordered among the different lipid systems studied.

References

1. Marquês, J. T.; de Almeida, R. F. M.; Viana, A. S. Lipid bilayers supported on bare and modified gold – Formation, characterization and relevance of lipid rafts. *Electrochimica Acta*. **2014**, *126*, 139-150.

2. Bott, A. W. Characterization of Films Immobilized on an Electrode Surface Using the Electrochemical Quartz Crystal Microbalance. *Current Separations* **1999**, *18*, 5.
3. de Almeida, R. F.; Borst, J.; Fedorov, A.; Prieto, M.; Visser, A. J. Complexity of lipid domains and rafts in giant unilamellar vesicles revealed by combining imaging and microscopic and macroscopic time-resolved fluorescence. *Biophys.J.* **2007**, *93*, 539-553.
4. Edholm, O.; Nagle, J. F. Areas of molecules in membranes consisting of mixtures. *Biophysical Journal* **2005**, *89*, 1827-1832.
5. Alwarawrah, M.; Dai, J. A.; Huang, J. Y. A Molecular View of the Cholesterol Condensing Effect in DOPC Lipid Bilayers. *J. Phys. Chem. B* **2010**, *114*, 7516-7523.
6. Loura, L. M. S.; de Almeida, R. F. M.; Coutinho, A.; Prieto, M. Interaction of peptides with binary phospholipid membranes: application of fluorescence methodologies. *Chem. Phys. Lipids* **2003**, *122*, 77-96.
7. Marsh, D. *Handbook of Lipid Bilayers*; Second ed.; CRC Press/Taylor & Francis Group: Boca Raton, 2013.
8. Jameson, D. M. In *New Trends in Fluorescence Spectroscopy*, Valeur, B.; Brochon, J.-C., Eds.; Springer/Verlag: Berlin, 2001; pp 35-58.
9. Valeur, B.; Berberan-Santos, M. N. *Molecular Fluorescence: Principles and Applications*; Second ed.; Wiley/VCH: New York, 2012; pp 569-571.